International Research Journal of Engineering and Technology (IRJET) e-ISSN: 2395-0056
Volume: 13 Issue: 06 | Jun 2026 www.irjet.net p-ISSN: 2395-0072

Cyclic Seismic Performance of Suicidal Hexagonal-Shaped Ductile Shear Panel in X-Bracing System Using ANSYS

Irshad Ebrahim[1], Dr. George K. George[2]

[1]M.Tech Scholar, [2]Professor Department of Civil Engineering, KMEA Engineering College, APJ Abdul Kalam Technological University, Edathala, Kerala, India

---

ABSTRACT-*Conventional X-braced structural frames are susceptible to brace buckling, pinched hysteresis loops, and premature failure under earthquake loading. Ductile Shear Panels (DSPs) inserted at brace intersections serve as sacrificial fuse elements designed to yield first, thereby protecting primary frame members from inelastic damage. This study investigates the cyclic seismic performance of an innovative Hexagonal Core (HC) honeycomb-shaped ductile shear panel embedded in an X-bracing system, analysed using ANSYS Workbench 2025 R2. Advanced nonlinear material models and large deformation analysis are employed to simulate the inelastic response under displacement-controlled cyclic loading following the FEMA SAC/BD-97 protocol. A total of fourteen finite element models are developed and analysed: two reference specimens BDSP-5 (stiffened braced ductile shear panel) and WOS (without stiffeners) validated against published experimental data, and twelve parametric HC models across three hexagonal cell sizes (100 mm, 200 mm, and 300 mm maximum horizontal span) with varying wall thicknesses. Key seismic performance indices evaluated include initial lateral stiffness (K_0), peak load capacity (Pm), yield load and displacement (Py, δy), ductility ratio (μ), hysteretic energy dissipation (Eh), equivalent viscous damping (ξeq), overstrength factor (RΩ), and Buckling Load Factor (BLF). The BDSP-5 validation model reproduced the experimental peak load within 1.83% and the maximum displacement within 3.13%. All twelve HC models demonstrated yield-governed behaviour with BLF ≥ 9.6. The 100HC-T16 configuration achieved the highest simultaneous values of stiffness (K_0 = 284.38 kN/mm), peak load (Pm = 1161.2 kN), ductility (μ = 16.48), and energy dissipation (Eh = 1093.6 kN·m), representing improvements of 3.77×, 3.6×, 3.1×, and 12.1× over BDSP-5 respectively. The results demonstrate that the suicidal hexagonal honeycomb shear panel constitutes a structurally superior alternative to conventional rectangular DSPs, delivering substantially enhanced strength, ductility, and energy dissipation without supplementary stiffening elements.*

Keywords-Hexagonal Core Honeycomb (HC); Ductile Shear Panel (DSP); X-bracing system; cyclic seismic performance; energy dissipation; finite element analysis; ANSYS Workbench; buckling load factor; hysteretic damping

I. INTRODUCTION

The field of structural engineering has experienced fundamental changes over recent decades, propelled by the growing imperative to construct buildings capable of surviving destructive seismic events. Earthquakes impose intricate, cyclic loading demands with pronounced nonlinear characteristics, routinely driving structural systems well beyond their elastic capacity thresholds. Contemporary seismic design philosophy accordingly prioritises controlled inelastic response, emphasising ductility and energy dissipation rather than reliance on purely elastic strength margins [1].

Ductile Shear Panels (DSPs) have gained recognition as a promising class of passive energy dissipation devices. These intentionally thin steel plates are designed to yield cyclically, channelling seismic energy through stable hysteretic deformation. When incorporated into braced frames at brace intersections, DSPs substantially elevate seismic performance by limiting the lateral force demand on beams, columns, and braces, enabling primary structure to remain largely undamaged following an earthquake [9].

Historically, DSPs have been fabricated as rectangular or square panels, frequently supplemented with stiffening ribs to postpone local buckling and sustain hysteretic stability. Contemporary research has expanded into alternative panel geometries to overcome stiffening requirements and amplify energy dissipation. The hexagonal shear panel represents one such geometric innovation, combining multiple load paths and superior local buckling resistance through its cellular architecture without supplementary stiffeners. The term 'suicidal' in this context denotes the intentional design philosophy the panel is engineered to yield first, sacrificing itself to safeguard the surrounding structural members.

Braced frames remain a primary lateral force-resisting system in steel structures. However, under reversed cyclic loading, conventional X-braced frames exhibit performance deficiencies: compression braces buckle abruptly causing severe stiffness deterioration, post-buckling energy dissipation is limited producing pinched hysteresis, and plasticity is localised increasing fracture risk [34]. The introduction of a replaceable DSP at the brace intersection reconstitutes the system as a fuse-

type mechanism, amplifying ductility and lowering post-earthquake repair costs [11].

The hexagonal honeycomb configuration, modelled after natural cellular structures, offers outstanding structural efficiency. A regular hexagonal tessellation yields multiple in-plane load paths, isotropic resistance to directional loading, and exemplary material utilisation per unit mass. The cellular architecture subdivides the enclosed area into compact individual cells, each with localised buckling resistance governed by the cell span and wall thickness rather than the overall panel dimensions, yielding Buckling Load Factors substantially greater than unity inherently [2].

This study quantifies the cyclic seismic performance of an X-bracing configuration incorporating a suicidal hexagonal-shaped DSP at the brace intersection, modelled and evaluated using ANSYS Workbench 2025 R2. Performance metrics are benchmarked against the conventional stiffened BDSP-5 and unstiffened WOS reference configurations, with particular emphasis on drift capacity, hysteretic stability, and energy dissipation.

II.LITERATURE REVIEW

Sun et al. [1] presented a landmark experimental programmer on the Braced Ductile Shear Panel system at one-third scale. Eight specimens examined the influence of panel thickness, dimensions, and stiffening rib configurations on cyclic response. Panels with closely spaced stiffening ribs gave fuller hysteresis loops and higher over strength ratios (above 3.0), while unstiffened panels exhibited characteristic pinching from shear buckling followed by tension field action. All specimens failed in the panel zone never in braces or frame validating the desired failure hierarchy.

Shahverdi Moghaddam et al. [2] investigated the large-deformation in-plane shear response of a composite hexagonal honeycomb core fabricated from fibreglass and phenolic resin using Digital Image Correlation. Cell wall geometric parameters were identified as primary regulators of shear stiffness, demonstrating that hexagonal cellular geometries possess inherently superior shear-carrying capacity.

Xiang et al. [4,5] studied cold-formed thin-walled steel frames with braced shear panel dampers in X- and K-shaped configurations. The K-shaped variant was repaired by replacing the shear panel within 35 minutes after a 1% drift test; repaired specimens exhibited near-identical cyclic response to the original, validating the replaceable fuse concept. Reducing aspect ratio and width-to-thickness ratio enhanced load capacity and energy dissipation.

Giannuzzi et al. [9] introduced the braced ductile shear panel as an innovative seismic-resistant framing system, demonstrating stable hysteretic behaviour and effective lateral displacement control under cyclic loading. Nakashima et al. [10] showed that low-yield steel shear panels develop stable wide hysteresis loops, enabling large plastic deformation without brittle failure.

The reviewed studies confirm that sacrificial fuse elements based on controlled shear yielding can achieve stable, high-ductility hysteretic behaviour. However, no research has been identified that investigates hexagonal or honeycomb core geometries specifically as ductile shear panels in seismic frames the present study directly addresses this research gap [1,2].

III. MATERIALS AND METHODOLOGY

A. Material Properties

All panel components are modelled using Q235B structural steel, while X-brace members and surrounding flange frame are assigned Q345B steel. Material properties are taken from the actual coupon test data reported by Sun et al. [1], which serve as the authoritative source for all material input values (Table I).

TABLE I. Material Properties of Q235B and Q345B Steels (Coupon Test Values)

Property	Q235B (Panel)	Q345B (Braces/Frame)
Yield Stress fy	281.5 MPa	331.22 MPa
Ultimate Stress fu	399.45 MPa	471.00 MPa
Young's Modulus E	2.03×10^5 MPa	2.03×10^5 MPa
Poisson's Ratio ν	0.3	0.3
Elongation at Fracture	33%	32%

A bilinear kinematic hardening model is used in all ANSYS simulations, defined by the yield stress and the elastic modulus, with a post-yield hardening slope computed from the ultimate stress and elongation data. The bilinear model was adopted for computational efficiency, as a multi linear model produced negligible differences in peak load values (< 2%) for the displacement amplitudes used in the SAC/BD-97 protocol.

B. Geometric Modelling

All models are developed in ANSYS Workbench 2025 R2. The surrounding frame geometry is identical for all fourteen models: a 1400 mm × 840 mm frame, with the shear panel at the brace intersection. For the HC series

models, the shear panel region is replaced by a hexagonal honeycomb core geometry. Three hexagonal cell size series are defined based on the maximum horizontal span: 300 mm, 200 mm, and 100 mm. Within each series, four wall thickness variants are modelled. The fourteen model designations are: BDSP-5 and WOS (validation); 300HC-T30, T25, T20, T15; 200HC-T25, T20, T15, T10; and 100HC-T16, T12, T8, T4.

C. Finite Element Formulation

The SOLID186 three-dimensional 20-node hexahedral element is used throughout. SOLID186 provides better accuracy than the 8-node SOLID185 element for bending-dominated responses and curved geometries, making it suitable for the hexagonal cell wall geometries in the HC models. Adaptive sizing with a target element size of 20 mm is applied, selected based on a mesh convergence study demonstrating that the 20 mm mesh produced peak load values within 1% of a 10 mm refinement mesh. The resulting mesh for BDSP-5 comprises 3,314 elements and 19,862 nodes.

D. Boundary and Loading Conditions

All six degrees of freedom are constrained at the base (fully fixed). At the top, only the lateral translational degree of freedom UX is free. Cyclic lateral loading is applied as a prescribed displacement following the FEMA SAC/BD-97 protocol, with drift amplitudes incrementally increasing from 0.375% to 6.0% story drift ratio. The maximum drift amplitude corresponds to a lateral displacement of 50.4 mm at 6% drift for the 840 mm panel height. The analysis is terminated when lateral resistance drops below 85% of peak load or when numerical divergence occurs.

E. Nonlinear Analysis Strategy

Geometric nonlinearity is enabled through the NLGEOM solver option, activating the updated Lagrangian large-deformation formulation. Automatic time-stepping is activated with an initial sub-step size of 1/50 of the peak displacement amplitude. Equilibrium is enforced through the Newton-Raphson iterative procedure with a force-based convergence tolerance of 0.1%. A ceiling of 1000 load steps per drift level is set to guarantee sufficient resolution of hysteresis loops.

F. Performance Parameter Calculations

The following seismic performance parameters are extracted from force-displacement hysteresis data: (i) Initial lateral stiffness $K_0 = F_1/\delta_1$ from the first loading cycle; (ii) Peak loads Pm^+ and Pm^- as maximum absolute force values; (iii) Yield load Py and displacement δy using the Equivalent Energy Method (EEM); (iv) Ductility ratio $\mu = \delta u/\delta y$ where δu corresponds to 85% load retention; (v) Hysteretic energy dissipation Eh as sum of enclosed hysteresis loop areas; (vi) Equivalent viscous damping $\xi eq = Eh/(4\pi \times Es)$; (vii) Overstrength factor $R\Omega = Pm,avg/Py$; and (viii) Buckling Load Factor $BLF = \tau cr/\tau y$ using Timoshenko plate buckling theory for cell walls.

IV. RESULTS AND DISCUSSION

A. Validation of FE Model BDSP-5

The BDSP-5 specimen from Sun et al. [1] is a stiffened braced ductile shear panel at one-third scale with panel dimensions 500 mm × 350 mm, plate thickness 3 mm, and closely spaced stiffening ribs. The ANSYS model produced a peak load of 326.88 kN (average of positive and negative peaks) at a maximum displacement of 16.80 mm. The experimental data reports a peak load of 321.00 kN at 16.29 mm displacement. The percentage variation in peak load is 1.83% and in maximum displacement is 3.13%, both within the ±5% acceptance criterion (Table II). BDSP-5 sustains wide, stable hysteresis loops with minimal pinching, confirming the adequacy of the modelling approach.

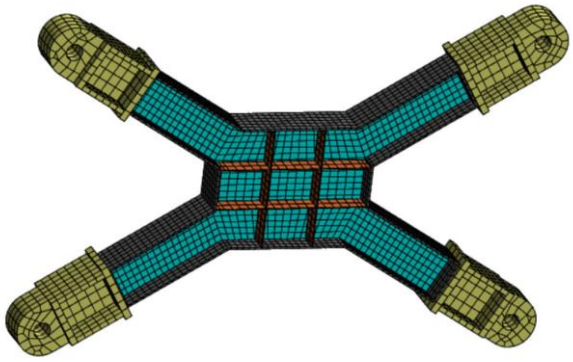

Fig. 1. ANSYS FE Mesh — BDSP-5 (3,314 elements, 19,862 nodes)

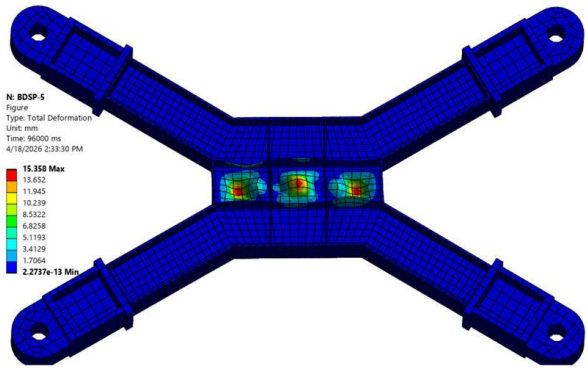

Fig. 2. Total Deformation Contour — BDSP-5 (Max = 15.36 mm)

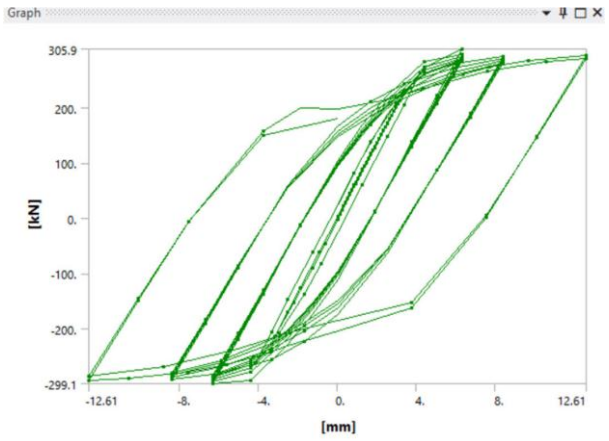

Fig. 3. Force–Displacement Hysteretic Curve BDSP-5

TABLE II. Comparison of BDSP-5 FEA Results with Experimental Data

Parameter	FEA (ANSYS)	Experimental	Variation (%)
Peak Load Pm,avg (kN)	326.88	321.00	1.83
Max Displacement Δmax (mm)	16.80	16.29	3.13

The WOS (without stiffeners) model achieves markedly higher ductility (μ = 11.91) and larger ultimate drift (2.97%), as tension field mechanism allows continued lateral force resistance over a wider displacement range. However, absolute lateral resistance (Pm,avg = 160.3 kN) is less than half that of BDSP-5, and ξeq = 0.270 is reduced due to the pinched loop shape. The BLF of 0.606 confirms elastic shear buckling initiates before panel yielding.

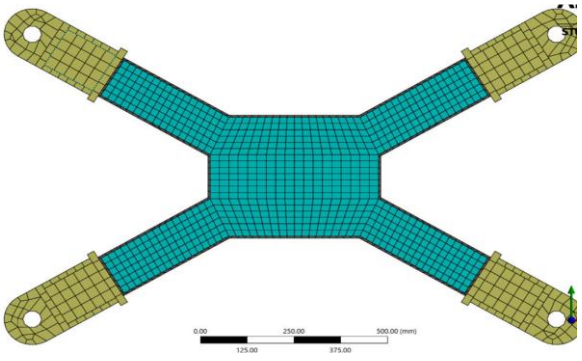

Fig. 4. ANSYS FE Mesh — WOS (Without Stiffeners)

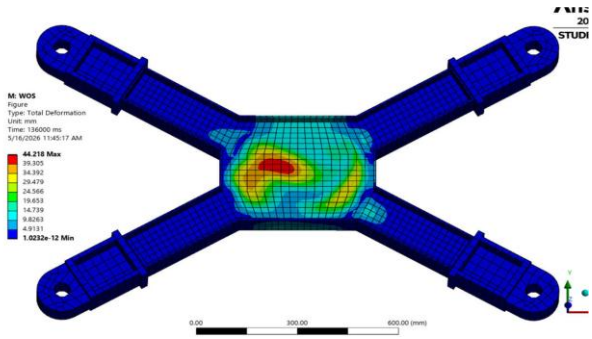

Fig. 5. Total Deformation Contour — WOS (Max = 44.22 mm)

B. 300 HC Series Results

All four 300 HC models sustained the maximum imposed drift of 6.0% without meeting the 85% load retention termination threshold, demonstrating exceptional displacement capacity. Yield-governed behaviour is confirmed by BLF values spanning 15.1 to 60.3, all far exceeding unity. Initial stiffness is strongly thickness-dependent, increasing 3.1-fold from 27.15 kN/mm (T15) to 83.55 kN/mm (T30). Peak lateral capacity spans 310.8 kN to 846.1 kN. Equivalent viscous damping values of 2.60–3.02 substantially exceed both BDSP-5 and WOS, reflecting distributed yielding across multiple cellular load paths.

C. 200 HC Series Results

The 200 HC series records substantially higher initial stiffness and peak loads than the 300 HC series at comparable thickness proportions. The 200HC-T25 specimen attains K_0 = 196.63 kN/mm and Pm,avg = 1054.8 kN. The 200HC-T20 configuration represents an outstandingly balanced performer, combining ductility ratio μ = 9.59 with the highest total energy dissipation in its series (Eh = 1027.3 kN·m) and the maximum equivalent viscous damping in the entire study (ξeq = 3.59). BLF values across the 200 HC series range from 15.1 (T10) to 94.2 (T25).

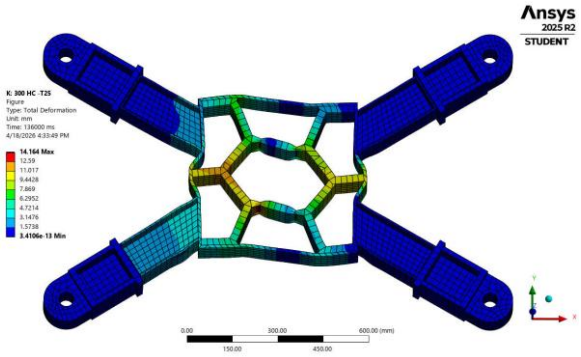

Fig. 6. Total Deformation Contour 300 HC-T25

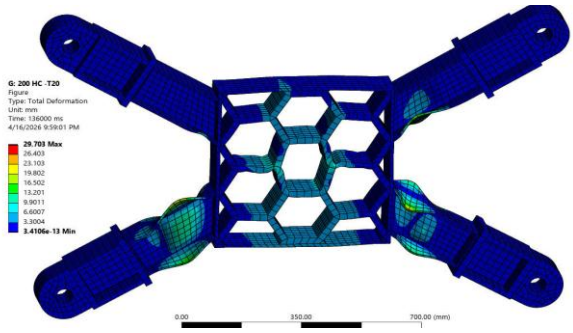

Fig. 7. Total Deformation Contour 200 HC-T20 (Outstanding Performer)

D. 100 HC Series Results

The 100 HC series delivers the most compelling seismic performance across the entire parametric study. The 100HC-T16 configuration achieves the highest values of four key parameters simultaneously: K_0 = 284.38 kN/mm (3.8× BDSP-5), Pm,avg = 1161.2 kN (3.6× BDSP-5), μ = 16.48 (3.1× BDSP-5), and Eh = 1093.6 kN·m (12.1× BDSP-5). The BLF of 154.3 for 100HC-T16 provides an exceptionally large margin against elastic buckling, guaranteeing full plastic yielding without pre-yield instability. Table III presents the seismic performance parameters for all 100 HC models.

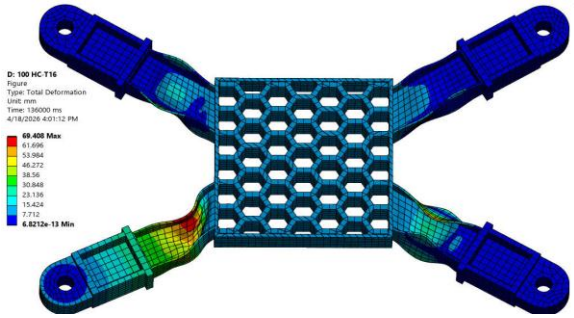

Fig. 8. Total Deformation Contour 100 HC-T16 (Optimal Configuration)

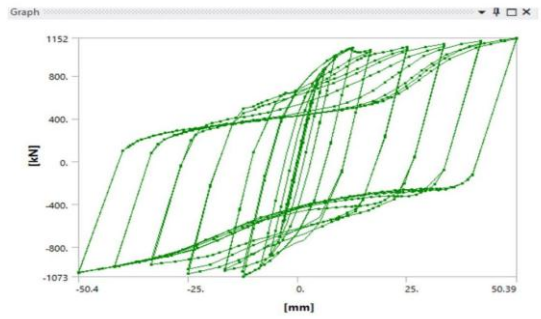

Fig. 9. Force–Displacement Hysteretic Curve 100 HC-T12

TABLE III. Seismic Performance Parameters 100 HC Series

Model	K_0 (kN/mm)	Pm,avg (kN)	μ,avg	Eh (kN·m)	ξeq	BLF
100HC-T16	284.38	1161.2	16.48	1093.6	2.86	154.3
100HC-T12	176.97	1112.7	10.70	1066.8	2.92	86.8
100HC-T8	71.76	611.9	7.89	601.4	3.09	38.6
100HC-T4	16.16	256.3	4.24	181.7	2.24	9.6

E. Consolidated Comparison of All 14 Models

Table IV presents the consolidated comparison of all fourteen models. Initial lateral stiffness spans 16.16 kN/mm (100HC-T4) to 284.38 kN/mm (100HC-T16), an 18-fold range. Within any given HC series, wall thickness is the primary stiffness driver; reducing cell span consistently elevates stiffness. All HC models with wall thickness ≥ 8 mm record higher initial stiffness than both reference specimens.

TABLE IV. Consolidated Comparison of All 14 Models

Model	K_0 (kN/mm)	Pm,avg (kN)	μ,avg	Eh (kN·m)	ξeq	RΩ
BDSP-5★	75.40	326.9	4.63	90.1	0.46	3.02
WOS★	92.40	160.3	11.91	243.8	0.27	1.90
300HC-T30	83.55	846.1	6.64	690.3	2.60	1.36
300HC-T25	66.48	576.8	7.75	553.6	3.02	1.34
300HC-T20	46.47	439.2	7.11	414.2	2.95	1.35
300HC-T15	27.15	310.8	5.87	281.6	2.87	1.35
200HC-T25	196.63	1054.8	6.27	486.6	2.87	1.38
200HC-T20★★	128.84	903.0	9.59	1027.3	3.59	1.34
200HC-T15	66.01	617.1	7.19	629.6	3.21	1.34
200HC-T10	48.74	366.6	4.64	146.7	2.42	1.34
100HC-T16★★	284.38	1161.2	16.48	1093.6	2.86	1.45
100HC-T12	176.97	1112.7	10.70	1066.8	2.92	1.43
100HC-T8	71.76	611.9	7.89	601.4	3.09	1.35
100HC-T4	16.16	256.3	4.24	181.7	2.24	1.34

★ Validation model ★★ Outstanding performer (best-in-class)

F. Buckling Load Factor Analysis

The BLF results unambiguously validate the hexagonal cell geometry as a yield-governed structural fuse mechanism. All twelve HC models record BLF values of at least 9.6, confirming cell wall yielding precedes local elastic buckling in every configuration. The WOS

reference records BLF = 0.606, confirming elastic buckling precedes yielding in the unbraced 3 mm flat panel. The BDSP-5 stiffened reference achieves BLF = 5.77 through the effective sub-panel sizing provided by its stiffening rib grid. The extreme BLF of 154.3 for 100HC-T16 establishes the 100 mm cell size as the most buckling-resistant configuration, with elastic buckling load more than 150 times the shear yield threshold.

G. Key Performance Trends

Peak loads range from 256.3 kN (100HC-T4) to 1161.2 kN (100HC-T16). The 100 HC series delivers the highest capacity, reflecting its compact cell geometry providing more cell walls per unit panel area. Even the 300HC-T30 model (846.1 kN) represents more than double the BDSP-5 peak load. Ductility ratios range from 4.24 to 16.48; the 100HC-T16 model achieves a drift ratio of 6.0% without significant strength degradation, far exceeding the 3% minimum for Special Moment Frames. Cumulative energy dissipation Eh ranges from 90.1 kN·m (BDSP-5) to 1093.6 kN·m (100HC-T16). Equivalent viscous damping ξeq spans 0.27 (WOS) to 3.59 (200HC-T20). Every HC model records substantially higher ξeq than both reference panels, confirming that pre-yield stability enforced by the high BLF of the cellular geometry produces fuller, less pinched hysteresis loops.

V. CONCLUSIONS

This study presents the first comprehensive finite element investigation of hexagonal core honeycomb ductile shear panels in X-bracing systems under cyclic seismic loading. The following conclusions are drawn from analysis of 9,317 total load steps across 14 ANSYS models:

1) Validation: The BDSP-5 numerical model reproduces the experimentally measured peak load with a deviation of only 1.83%, and maximum displacement within 3.13%, both within the ±5% acceptance criterion, validating the FE modelling approach.

2) Buckling Load Factor: All twelve HC models demonstrate yield-governed behaviour with BLF ≥ 9.6; the maximum BLF of 154.3 is recorded for 100HC-T16. The hexagonal cell geometry inherently guarantees yield-governed fuse behaviour across the full wall thickness range, without supplementary stiffening.

3) Initial Stiffness: K_0 ranges from 16.16 kN/mm (100HC-T4) to 284.38 kN/mm (100HC-T16), an 18-fold range. The 100HC-T16 model achieves 3.77× the initial stiffness of BDSP-5.

4) Load Capacity: Peak load Pm,avg spans 256.3 kN to 1161.2 kN. Both 100HC-T16 and 100HC-T12 exceed 1100 kN, more than 3.4× the BDSP-5 capacity. Even the thinnest 300 HC model (310.8 kN) matches BDSP-5 peak load without stiffening.

5) Ductility: Ductility ratios μ,avg range from 4.24 to 16.48. All HC models reach drift ratios of δu/h = 6.0% without meeting the strength degradation criterion, confirming seismic suitability.

6) Energy Dissipation: Cumulative hysteretic energy Eh ranges from 90.1 kN·m (BDSP-5) to 1093.6 kN·m (100HC-T16). The 100HC-T16 and 200HC-T20 configurations exceed BDSP-5 energy dissipation by more than twelve times.

7) Equivalent Viscous Damping: ξeq ranges from 0.27 (WOS) to 3.59 (200HC-T20). Every HC model records substantially higher ξeq than both reference panels.

8) Optimal Configuration: The 100HC-T16 model represents the optimal overall performer. The 200HC-T20 model, with the highest ξeq of the study, offers the best trade-off between energy dissipation efficiency and geometric compactness.

The results demonstrate that hexagonal honeycomb core shear panels constitute a structurally superior alternative to conventional rectangular DSPs, delivering substantially enhanced strength, ductility, and energy dissipation without supplementary stiffening elements. These findings form a strong foundation for future experimental verification and the formulation of code-based design expressions for HC shear panel seismic systems. Future research should focus on:

(i) experimental verification at structural scale;
(ii) optimisation of cell size-to-thickness ratios for target performance levels; and
(iii) soil-structure interaction studies.

ACKNOWLEDGEMENT

The authors gratefully acknowledge the guidance and support of Prof. Dr. George K. George, Project Supervisor and PG Coordinator, Department of Civil Engineering, KMEA Engineering College. The authors also thank Dr. Biji Chinnamma Thomas, Head of Department, and Dr. Amar Nishad T.M., Principal, KMEA Engineering College. This research was conducted as part of the M.Tech programme in Computer Aided Structural Engineering at APJ Abdul Kalam Technological University, Kerala.

REFERENCES

1) G. Sun, C. Bao, W. Liu, Y. Fang, "Cyclic behavior of an innovative braced ductile thin shear panel," Structures, 2021. https://doi.org/10.1016/j.istruc.2021.03.075

2) H. Shahverdi Moghaddam et al., "In-plane shear response of a composite hexagonal honeycomb core under large deformation," Composite Structures, 2021.

3) G. Sun, Yu, "Cyclic testing of an innovative self-centering X-braced ductile shear panel," 2021.

4) Y. Xiang et al., "Experimental research on seismic performance of cold-formed thin-walled steel frames with braced shear panel," Thin-Walled Structures, 2023.

5) Y. Xiang et al., "Study on seismic performance of cold-formed thin-walled steel frame with K-shaped braced shear panel," Thin-Walled Structures, 2023.

6) M. Iqbal et al., "Development of mortar filled honeycomb sandwich panels for resistance against repeated ballistic impacts," Journal of Materials Research and Technology, 2023.

7) N.A.A. Hamza et al., "Experimental and numerical study of effecting core configurations on static and dynamic behavior of honeycomb plate," Defence Technology, 2024.

8) M. Ahsanfar, S.A. Galehdari, "Optimum design for graded honeycomb as energy absorber device in elevator cabin," Procedia Engineering, 2017.

9) D. Giannuzzi et al., "Braced Ductile Shear Panel: New Seismic-Resistant Framing System," Journal of Structural Engineering, ASCE, 2014.

10) M. Nakashima et al., "Energy dissipation behaviour of shear panels made of low-yield steel," Earthquake Engineering & Structural Dynamics, vol. 23, no. 12, pp. 1299-1313, 1994.

11) S. Soltani et al., "Numerical Investigation of Pinned Fuse with Simple Replacing in Steel Eccentrically Braced Frames," Journal of Rehabilitation in Civil Engineering, 2024.

12) Astaneh-Asl, "Seismic behavior and design of steel shear walls," Structural Steel Educational Council, 2001.

13) J.W. Berman, M. Bruneau, "Experimental investigation of light-gauge steel plate shear walls," Journal of Structural Engineering, ASCE, vol. 129, no. 11, pp. 1538-1546, 2003.

14) R.G. Driver et al., "Cyclic test of four-story steel plate shear wall," Journal of Structural Engineering, ASCE, vol. 124, no. 2, pp. 112-120, 1998.

15) A. M. Elgaaly et al., "Post-buckling behavior of steel plates in shear," Journal of Structural Engineering, ASCE, vol. 119, no. 2, pp. 588-605, 1993.

16) A. Farzampour, "Nonlinear behavior of steel shear panels under cyclic loading," Structures, vol. 20, pp. 635-645, 2019.

17) R. Sabelli et al., "Seismic demands on steel braced frame buildings with buckling-restrained braces," Engineering Structures, vol. 25, no. 5, pp. 655-666, 2003.

18) D. Vian, M. Bruneau, "Steel plate shear walls for seismic design and retrofit," Journal of Constructional Steel Research, vol. 61, no. 11, pp. 1539-1556, 2005.

19) T.M. Roberts, S. Sabouri-Ghomi, "Hysteretic characteristics of unstiffened perforated steel plate shear panels," Thin-Walled Structures, vol. 14, no. 2, pp. 139-151, 1991.

20) M.H. Kharrazi, C.E. Ventura, "Performance of unstiffened steel shear panels under cyclic loads," Earthquake Engineering and Structural Dynamics, vol. 35, no. 1, 2006.

21) R. Tremblay, "Inelastic seismic response of steel bracing members," Journal of Constructional Steel Research, vol. 58, no. 5-8, pp. 665-701, 2002.

22) A. Farzampour, M.R. Eatherton, "Cyclic behavior of steel slit shear walls," Journal of Constructional Steel Research, vol. 144, pp. 273-284, 2018.

23) E. Alavi, F. Nateghi, "Experimental study on steel slit shear walls," Journal of Constructional Steel Research, vol. 89, pp. 9-20, 2013.

24) Q. Zhou, Y. Zhang, "Numerical study of corrugated steel shear panels under cyclic loading," Thin-Walled Structures, vol. 107, pp. 335-347, 2016.

25) Q. Zhao, A. Astaneh-Asl, "Cyclic behavior of traditional and innovative steel plate shear walls," Journal of Structural Engineering, ASCE, vol. 130, no. 8, pp. 1187-1196, 2004.